Supporting Information

Seeded Growth of $Cu_{2-x}Se$ Nanocrystals and Their Size-dependent Phototherapeutic Effect

Xianguang Ding, [†,‡] *Dongdong Fu,* [†,‡,§] *Ye Kuang,* [†] *Yu Zou,* [†] *Xiuzhu Yang,* [†,§] *Liangzhu Feng,* [⊥] *Xia Sun,* [†] *Haiyan Wu,* [†] *and Jiang Jiang** [†]

[†] *i*-Lab and Division of Nanobiomedicine, CAS Key Laboratory of Nano-Bio Interface, CAS Center for Excellence in Nanoscience, Suzhou Institute of Nano-Tech and Nano-Bionics, Chinese Academy of Sciences, Suzhou 215123, China

[§] University of Chinese Academy of Sciences, Beijing, China 100049

[⊥] *Institute of Functional Nano & Soft Materials (FUNSOM), Jiangsu Key Laboratory for Carbon-Based Functional Materials & Devices, Soochow University, 199 Ren'ai Road, Suzhou 215123, China*

Corresponding author:

* jjiang2010@sinano.ac.cn

Calculation of the mass attenuation coefficient

2 mL of various concentration NPs solution was loaded into a cuvette and the corresponding solution absorption spectra were taken. According to Beer-Lambert law $A = \alpha_m CL$, where A is the solution absorbance, L = 1 cm is the light pathlength, C is the mass concentration (g/L), and α_m is the mass extinction coefficient. From the measured Cu concentration (C_{Cu}), the converted mass concentration of $Cu_{2-x}Se$ is then equal to:

$$C_{Cu_{2-x}Se} = C_{Cu} \cdot \frac{(2-x)m_{Cu} + m_{Se}}{(2-x)m_{Cu}}$$

with m_{Cu} and m_{Se} being the atomic mass of the elements.

The corresponding nanoparticle molar extinction coefficient was then calculated based on the above obtained mass attenuation coefficient. First, single nanocrystal mass is obtained by the following equation:

$$m_{nanocrystal} = \rho \cdot \frac{4}{3}\pi r^3$$

where ρ is the density of berzelianite at 6.84 g/cm^3, and r is the nanocrystal radius. Then, the molar extinction coefficient is calculated from the obtained mass extinction coefficient as:

$$\alpha_M = \alpha_m \cdot \frac{m_{nanocrystal}}{1\ g} \cdot 6.022 \times 10^{23}$$

Supplementary Figures

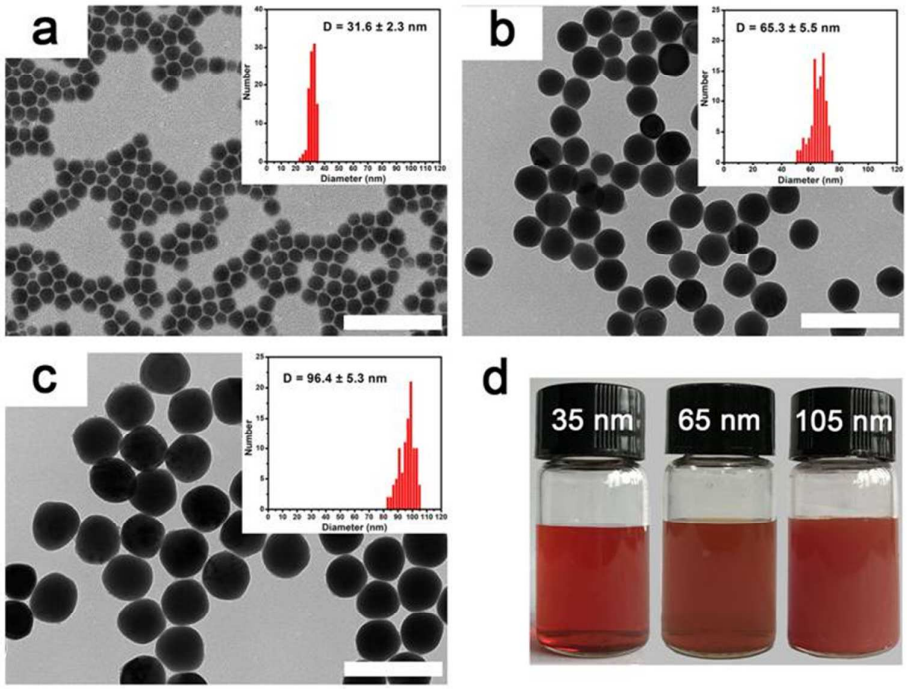

Figure S1. (a-c) TEM images of various sized Se NPs with size distribution histogram presented in the insets, all the scale bars represent 200 nm; (d) solution visual appearance of different sized Se NP dispersions.

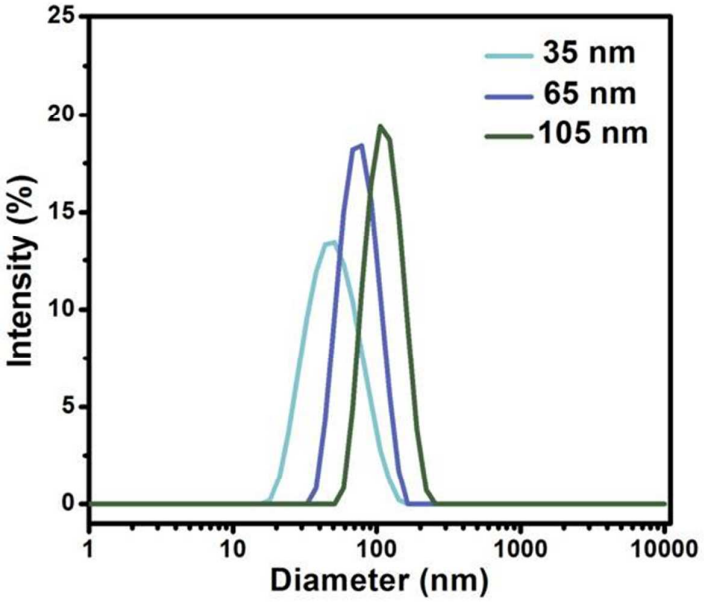

Figure S2. Hydrodynamic diameters of different sized $Cu_{2-x}Se$ NPs of PSS capping measured by DLS.

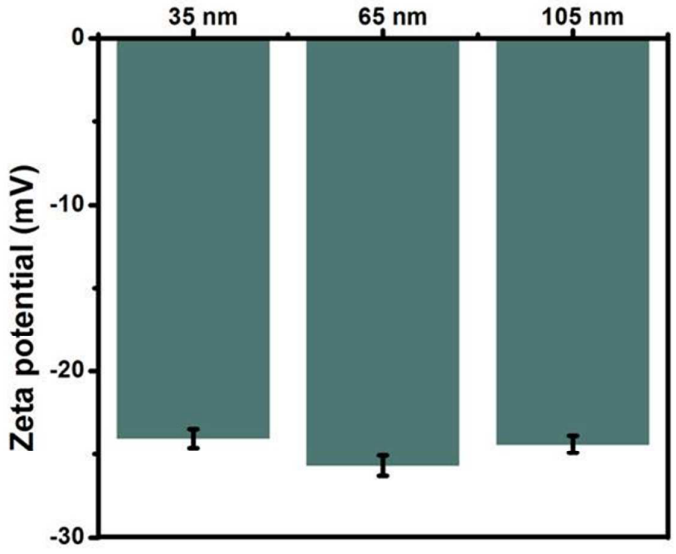

Figure S3. Zeta potential of different sized $Cu_{2-x}Se$ NPs with PSS capping.

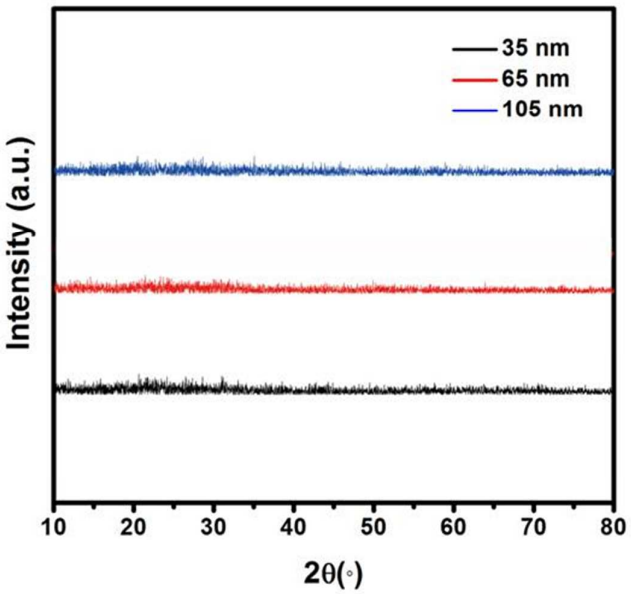

Figure S4. X-ray diffraction patterns of various sized Se NPs with no obvious diffraction peaks.

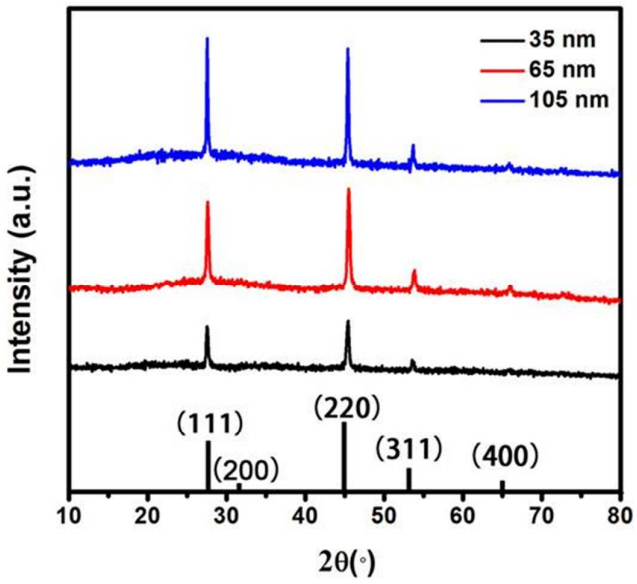

Figure S5. X-ray diffraction patterns of crystalline $Cu_{2-x}Se$ NPs of various sizes, which are all in cubic berzelianite phase (JCPDS 71-0044).

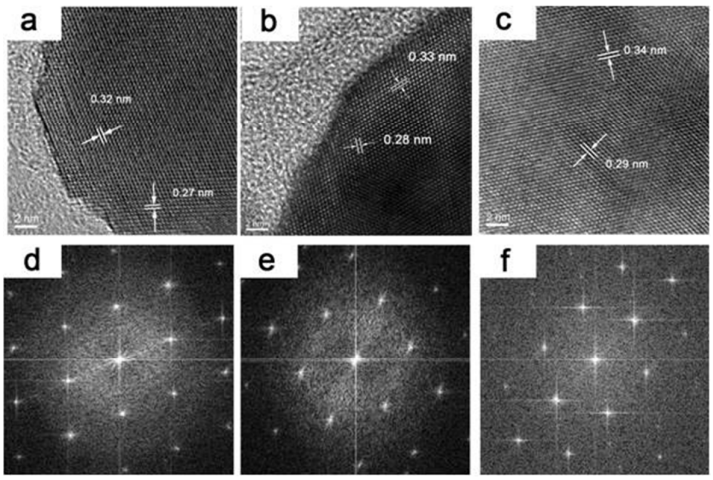

Figure S6. (a-c) High resolution TEM images of 35, 65, and 105 nm $Cu_{2-x}Se$ NPs, and (d-f) the corresponding electron diffraction patterns. The lattice spacing value of ~ 0.29 nm and 0.33 nm matches well with the {220} and {111} lattice planes of berzelianite $Cu_{2-x}Se$, respectively.

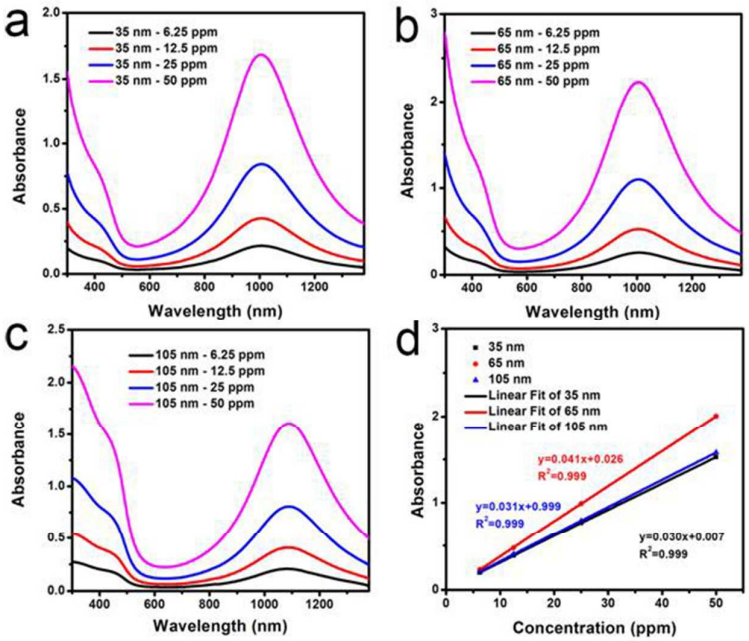

Figure S7. UV-vis-NIR absorption spectra of (a) 35 nm, (b) 65 nm, and (c) 105 nm diameter $Cu_{2-x}Se$ NPs aqueous dispersion with various concentration of Cu^{2+} (6.25, 12.5, 25, 50 and 80 ppm); (d) plots of linear fit to the absorbance at 1064 nm versus concentration for aqueous dispersion of 35, 65, and 105 nm $Cu_{2-x}Se$ NPs.

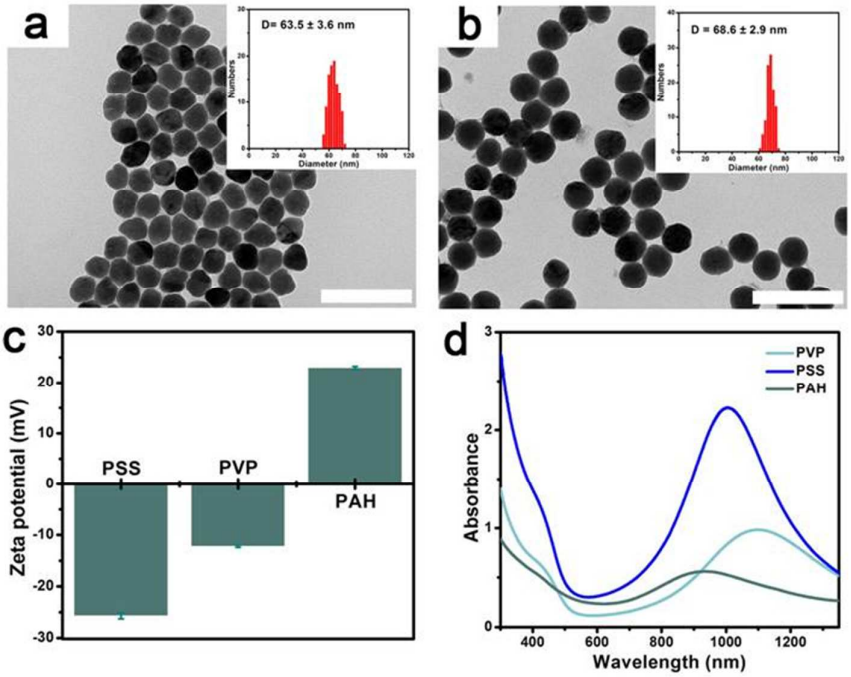

Figure S8. TEM images of 65 nm diameter $Cu_{2-x}Se$ NPs synthesized with (a) PVP and (b) PAH, with the size histogram shown in the inset, and the scale bars represent 200 nm; (c) zeta-potential of three $Cu_{2-x}Se$ NPs with different surfactant molecules; (d) absorption spectra of PVP and PAH capped $Cu_{2-x}Se$ NPs.

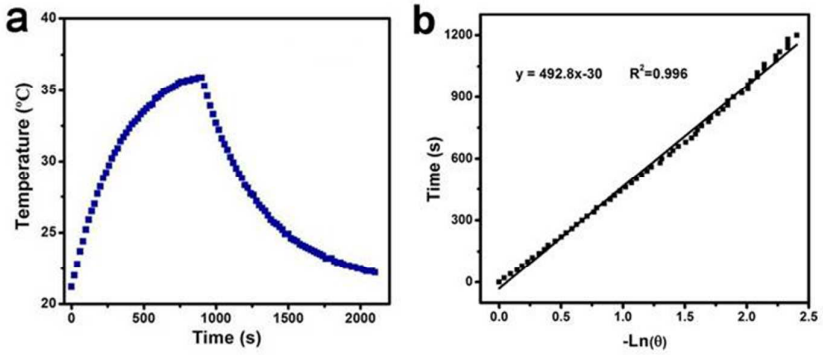

Figure S9. (a) Photothermal cooling profile of the 65 nm $Cu_{2-x}Se$ nanocrystal solution, and (b) determination of the time constant for heat transfer from the system using linear regression of the cooling profile in (a).

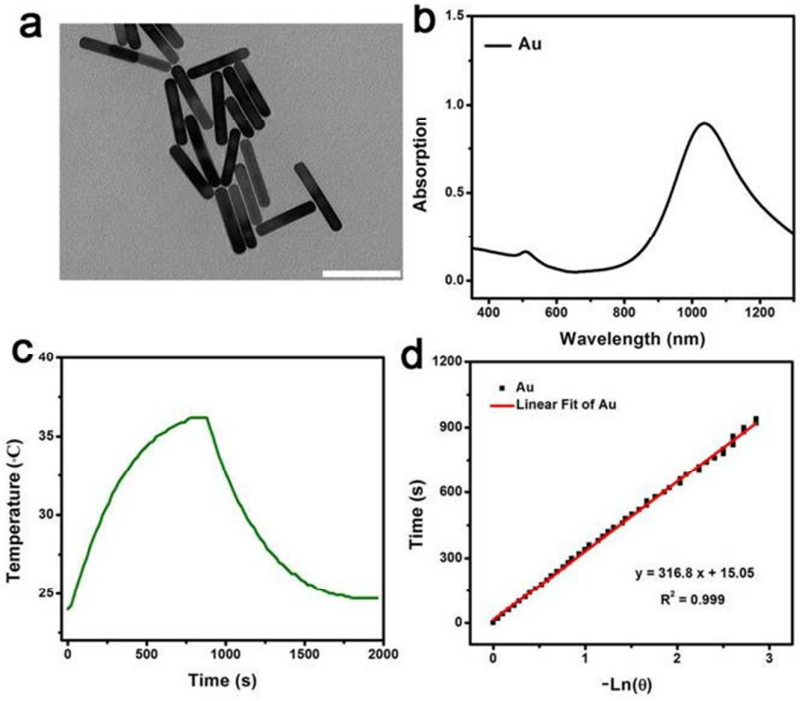

Figure S10. (a) TEM image (scale bar 100 nm), (b) optical absorbance, and (c) photothermal cooling profile of the Au NR solution; (d) determination of the time constant for heat transfer from the system using linear regression of the cooling profile in (c).

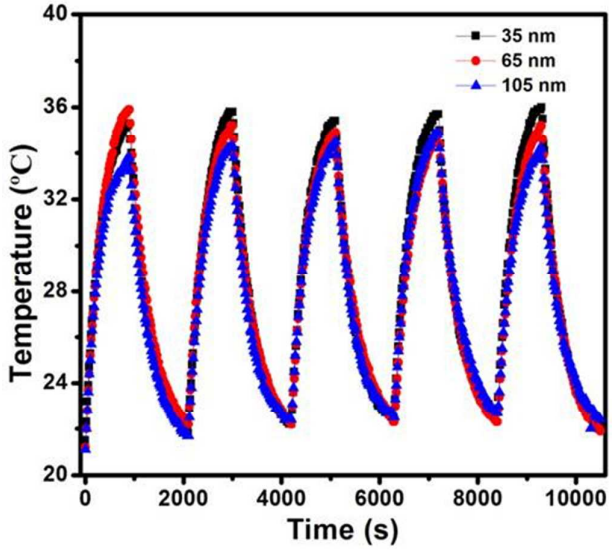

Figure S11. Temperature variations of as-prepared $Cu_{2-x}Se$ NPs (50 ppm) under irradiation by 1064 nm laser at a power density of 0.75 W/cm^2 for 5 cycles (15 min irradiation for each cycle).

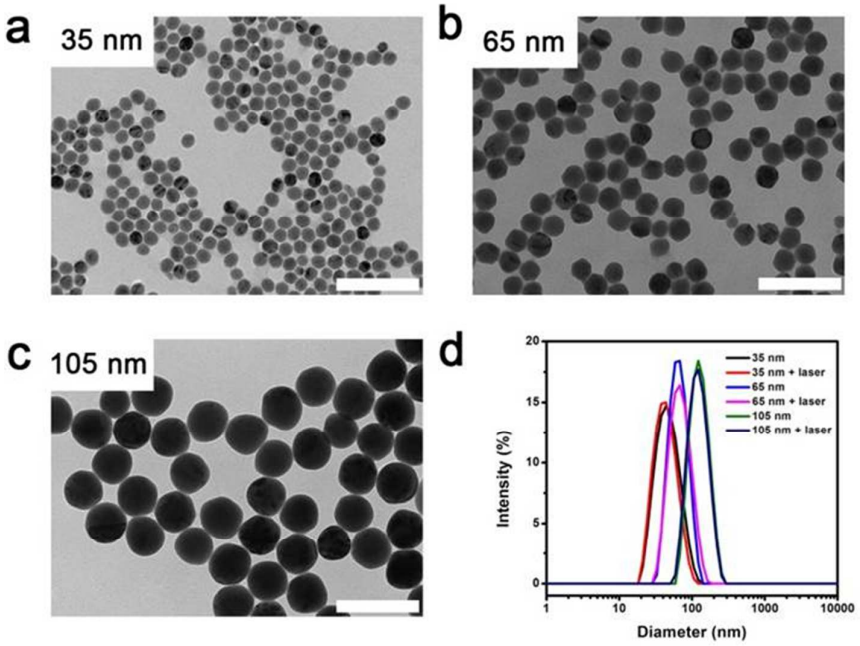

Figure S12. (a-c) TEM images of different sized $Cu_{2-x}Se$ NPs (scale bars 200 nm) after irradiation by 1064 nm laser at a power density of 0.75W/cm^2 for 30 min, and (d) their corresponding hydrodynamic diameters before and after laser irradiation.

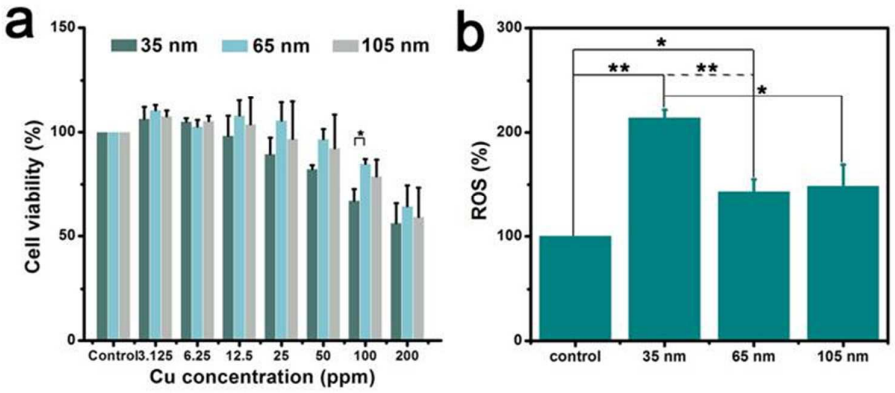

Figure S13. (a) HUVEC cell viabilities after incubation with $Cu_{2-x}Se$ NPs of different concentrations; (b) generation of ROS in HUVEC cells incubated with different sized $Cu_{2-x}Se$ NPs (100 ppm).

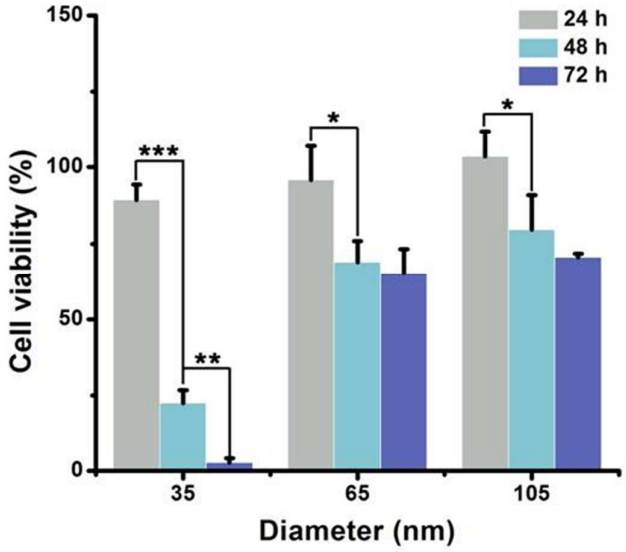

Figure S14. CT26 cell viability after being incubated with 50 ppm $Cu_{2-x}Se$ NPs for various time, with * stands for $P < 0.05$, ** stands for $P < 0.01$, and *** stands for $P < 0.001$.

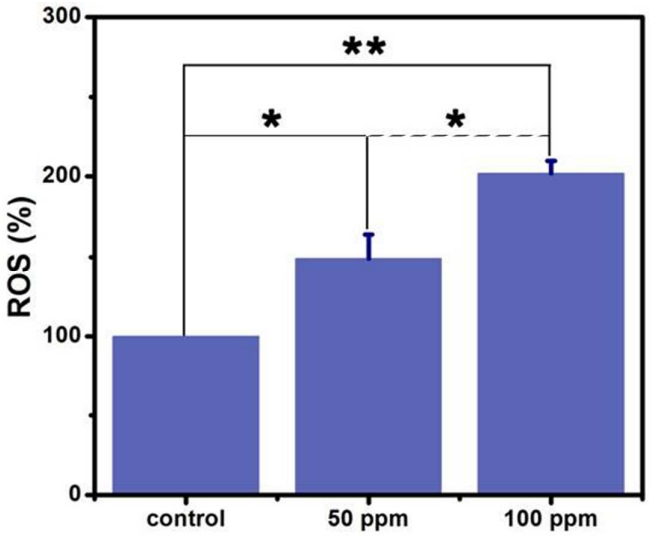

Figure S15. Generation of ROS in a dose-dependent manner.

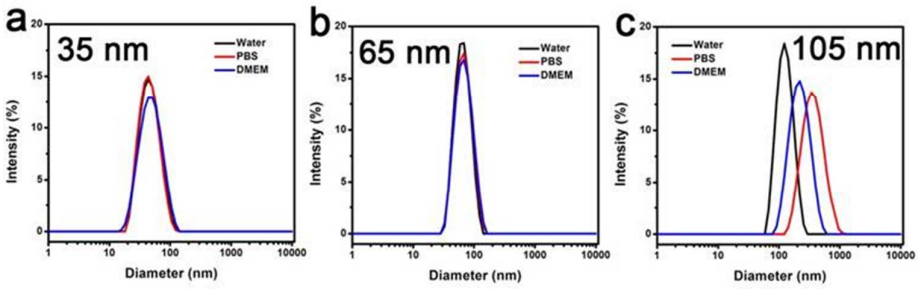

Figure S16. Hydrodynamic sizes of (a) 35 nm, (b) 65 nm, and (c) 105 nm diameter PSS capped $Cu_{2-x}Se$ NPs in different dispersing solvent such as water, PBS, and DMEM with 10% FBS.

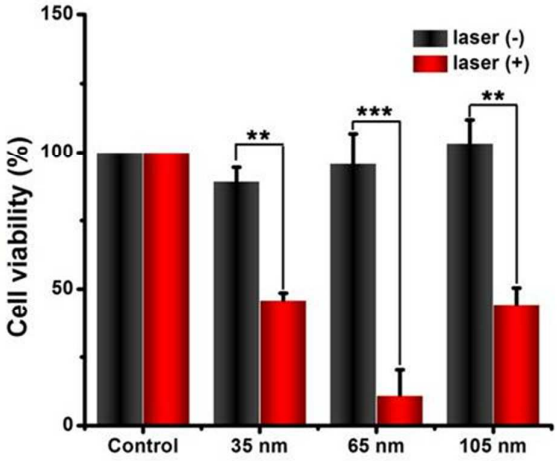

Figure S17. MTT viability assays of CT26 cells after incubating with various sized $Cu_{2-x}Se$ NPs (50 ppm) without and with irradiation of a 1064 nm laser (1W/cm^2, 10 min). * stands for $P < 0.05$, ** stands for $P < 0.01$, and *** stands for $P < 0.001$.

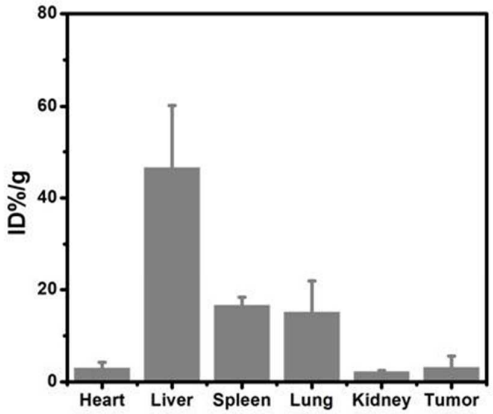

Figure S18. Biodistribution of $Cu_{2-x}Se$ NPs 24 h post i.v. injection measured by ICP.

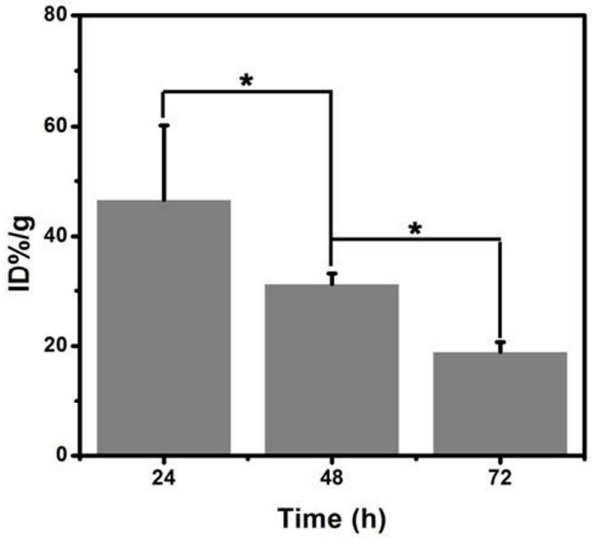

Figure S19. Accumulated amount of $Cu_{2-x}Se$ NPs in liver at different time post i.v. injection determined by ICP measurement.

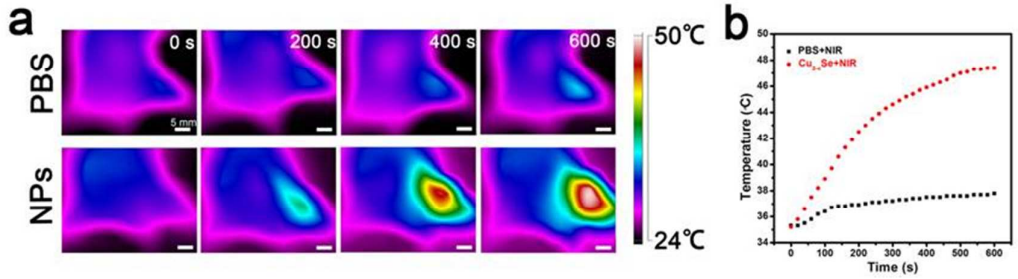

Figure S20. (a) Thermal images of CT26 tumor-bearing mice after intratumoral injection of PBS and 65 nm $Cu_{2-x}Se$ NPs (100 μL of 100 ppm) under the 1064 nm laser irradiation for 10 min (1 W/cm^2), scale bars represent 5 mm; (b) recorded temperature changes at mice tumor site during laser irradiation.

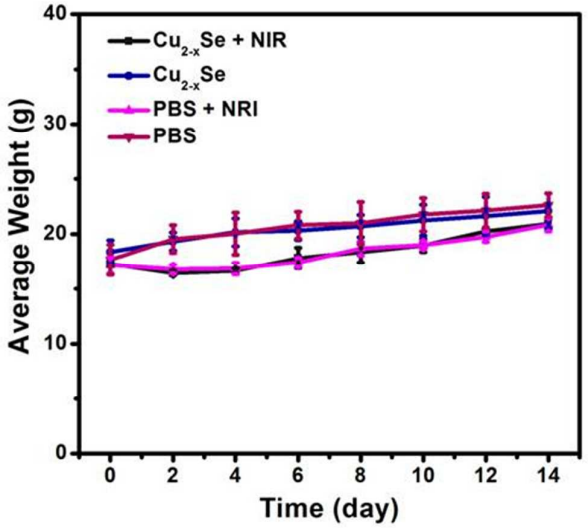

Figure S21. The body weight variation of CT26 tumor-bearing mice after different treatments.

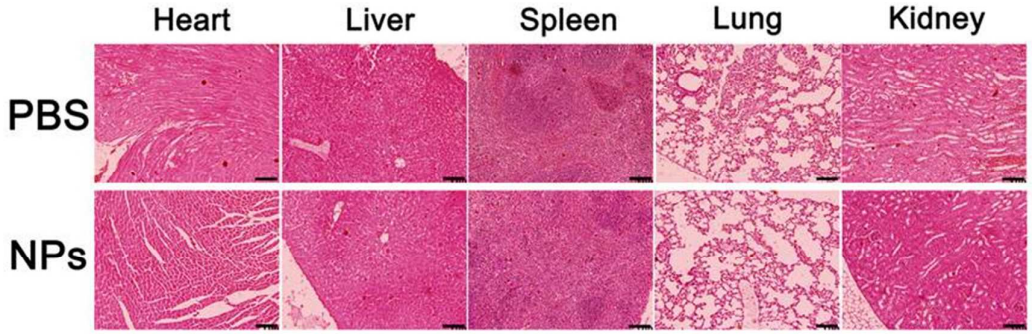

Figure S22. H&E stained slices of major organs in mice 14 days after $Cu_{2-x}Se$ injection and PTT treatment, with scale bars represent 100 μm. No obvious organ damage or inflammatory lesions were observed compared to control group.

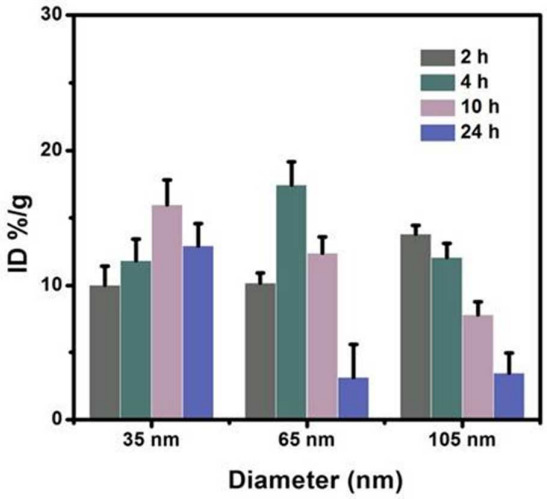

Figure S23. Accumulated $Cu_{2-x}Se$ NPs of various sizes at different time post i.v. injection measured by ICP.